Title

Negative affect and craving during abstinence from smoking are both linked to default mode network connectivity.

Authors

Tabibnia, Golnaz
Ghahremani, Dara
Pochon, Jean-Baptiste
et al.

Publication Date

2023-08-01

DOI

10.1016/j.drugalcdep.2023.109919

Peer reviewed

HHS Public Access

Author manuscript

Drug Alcohol Depend. Author manuscript; available in PMC 2024 August 01.

Published in final edited form as:

Drug Alcohol Depend. 2023 August 01; 249: 109919. doi:10.1016/j.drugalcdep.2023.109919.

Negative affect and craving during abstinence from smoking are both linked to default mode network connectivity

Golnaz Tabibnia[a], **Dara G. Ghahremani**[b], **Jean-Baptiste F. Pochon**[b], **Maylen Perez Diaz**[b], **Edythe D. London**[b]

[a]Department of Psychological Science, University of California, Irvine, CA, USA.

[b]Department of Psychiatry and Biobehavioral Sciences, Semel Institute for Neuroscience and Human Behavior, University of California, Los Angeles, CA, USA.

Abstract

Background: Negative affect and craving during abstinence from cigarettes predict relapse. Therefore, understanding their neural substrates may guide development of new interventions. Negative affect and craving have traditionally been linked to functions of the brain's threat and reward networks, respectively. However, given the role of default mode network (DMN), particularly the posterior cingulate cortex (PCC), in self-related thought, we examined whether DMN activity underlies both craving and negative affective states in adults who smoke.

Methods: 46 adults who smoke abstained from smoking overnight and underwent resting-state fMRI, after self-reporting their psychological symptoms (negative affect) and craving on the Shiffman-Jarvik Withdrawal Scale and state anxiety (negative affect) on the Spielberger State-Trait Anxiety Inventory. Within-DMN functional connectivity using 3 different anterior PCC seeds was tested for correlations with self-report measures. Additionally, independent component analysis with dual regression was performed to measure associations of self-report with whole-brain connectivity of the DMN component.

Results: Craving correlated positively with connectivity of all three anterior PCC seeds with *posterior* PCC clusters (p_{corr}<0.04). The measures of negative affective states correlated positively with connectivity of the DMN component to various brain regions, including posterior PCC (p_{corr}=0.02) and striatum (p_{corr}<0.008). Craving and state anxiety were correlated with connectivity of an overlapping region of PCC (p_{corr}=0.003). Unlike the state measures, nicotine dependence and trait anxiety were not associated with PCC connectivity within DMN.

Conclusions: Although negative affect and craving are distinct subjective states, they appear to share a common neural pathway within the DMN, particularly involving the PCC.

Keywords

Tobacco Use Disorder; nicotine; emotion; brain imaging; default mode network; withdrawal

Corresponding author: Golnaz Tabibnia, Department of Psychological Science, University of California, Irvine, 4201 Social and Behavioral Sciences Gateway, Irvine, CA 92697 USA, tabibnia@uci.edu.

1. Introduction

One of the greatest public health threats on record, smoking is linked to more than 8 million deaths globally each year (WHO, 2020). In the United States, about 55% of adults who smoke make a serious attempt to quit each year (Creamer et al., 2019; Gitchell et al., 2017). Of those, >92% fail to maintain abstinence beyond 6 months (Creamer et al., 2019). Chief among reasons for lapses are negative affect (e.g., anxiety, psychological withdrawal) and craving (Messer et al., 2018; Piper et al., 2011; Sinha, 2011; Zhou et al., 2009). With the advent of new intervention tools, including targeted brain stimulation, a better understanding of the neural substrates underlying negative affect and craving during abstinence can help address the problem of relapse.

Clinical neuroscience research has often focused on function of the reward network and the threat network in addiction and mental health broadly (Nelson et al., 2013; Tabibnia, 2020). For example, clinical depression has been characterized with dampened response in the reward network and heightened response in the amygdala and hypothalamic-pituitary-adrenal axis (Charney, 2004), whereas Tobacco Use Disorder (TUD) may involve normal threat response and aberrant reward response (Kunas et al., 2021). Similarly, craving has classically been associated with reward-related circuitry (Volkow and Morales, 2015) and anxiety with threat-related circuitry (Tye et al., 2011).

More recently, the default mode network (DMN) has emerged as another network that is relevant across mental health disorders (Tabibnia, 2020; Whitfield-Gabrieli and Ford, 2012), including TUD and other substance use disorders (Zhang and Volkow, 2019). The DMN is a distributed neural network involved in several functions, notably self-referential thought, such as thinking about one's past or future (Andrews-Hanna et al., 2014; Buckner and DiNicola, 2019). It tends to be active when a person is not engaged in tasks that demand externally-focused attention – i.e., during a wakeful "resting state" (Buckner and DiNicola, 2019; Raichle et al., 2001). Resting state functional connectivity (RSFC) in the DMN is associated with multiple processes, including negative subjective states (Lehmann et al., 2016; Li et al., 2020; Zhang et al., 2020; Zhou et al., 2020) . For example, hyperconnectivity and hyperactivation of the core regions of DMN, particularly posterior cingulate cortex (PCC) and medial prefrontal cortex (MPFC), have been linked with rumination and negative mood (Christoff et al., 2016; Zhou et al., 2020).

The first aim of the current study was to examine the role of the DMN in negative affect and craving during withdrawal from smoking. In people who smoke, RSFC within DMN during abstinence is stronger than after smoking (Ding and Lee, 2013; Huang et al., 2014; Janes et al., 2014; Li et al., 2017; Zhao et al., 2019) and stronger than in people who do not smoke (Huang et al., 2014; Vergara et al., 2017). In particular, early abstinence may increase RSFC in PCC and other DMN regions (Li et al., 2017). However, it is unclear whether RSFC within DMN is related to craving and negative affective states during abstinence. Previous studies have shown positive correlations of RSFC within DMN with cigarette craving (Huang et al., 2014; Janes et al., 2014; Zhao et al., 2019) and withdrawal (Cole et al., 2010). However, these studies had small sample sizes (Cole et al., 2010; Huang et al., 2014; Janes et al., 2014) ($n<18$) or did not include female participants (Zhao et al., 2019).

No study has evaluated the role of DMN RSFC in negative affective states, such as anxiety, during withdrawal from smoking.

The second aim of this study was to examine the similarity of pathways underlying negative affective states and craving. Craving and negative affect are often associated with one another (Fatseas et al., 2018; Giuliani and Berkman, 2015; Knapp et al., 2021; Watson et al., 2018; Wolitzky-Taylor and Schiffman, 2019) and may both contribute to substance use and relapse (Fatseas et al., 2018; Killen and Fortmann, 1997; Leventhal and Zvolensky, 2015; Piper et al., 2011; Watson et al., 2018); therefore, a similar mechanism may underlie both. Furthermore, anxiety and cigarette smoking tend to be comorbid (Leventhal and Zvolensky, 2015) and may have overlapping psychological mechanisms (Ameringer and Leventhal, 2010; Brewer and Roy, 2021). However, a common neural basis of craving and negative affective states within DMN remains unreported. By moving away from the dichotomy of threat and reward and towards a more unifying approach, demonstrating that a common mechanism underlies both subjective states could help identify therapies that address more than one symptom or that are transdiagnostic.

Using secondary analysis of data from a sample of 46 men and women, we tested the hypotheses that after overnight abstinence from smoking 1) DMN RSFC is associated specifically with craving and negative affective states, and 2) a similar pathway underlies both subjective states, as indicated by correlated self-report measures and partially overlapping DMN connectivity patterns. To mitigate issues related to analytical variability (Botvinik-Nezer et al., 2020), we implemented two different analysis pipelines. Taking a confirmatory approach, we used seed-based analyses to identify correlations between subjective states and RSFC of PCC within DMN. These analyses focused on connectivity *within* DMN, because within-network RSFC is more predictive of smoking status than between-network RSFC (Pariyadath et al., 2014). The PCC was selected as seed because of its involvement in negative subjective states (Berman et al., 2014; Renner et al., 2017; Zhang et al., 2020; Zhou et al., 2020) and smoking abstinence (Li et al., 2017), and because of its potential as a therapeutic target in both anxiety and substance use disorders (Brewer and Garrison, 2014). In a second, more exploratory approach, we used independent component analysis (ICA) with dual regression in whole-brain analyses to identify brain regions in which RSFC within DMN correlates with subjective states.

2. Material and methods

2.1. Participants

One hundred seventy-nine participants who responded to online and print advertisements attended an in-person screening session. Fifty-one participants met all entry criteria and completed study procedures. Of these, five were excluded due to missing self-report data, excessive motion during scanning, and/or unverified overnight abstinence, resulting in a final sample of 46 individuals who endorsed daily smoking.

Inclusion criteria were age of 18–45 years, general good health, self-report of smoking at least four cigarettes per day for at least one year, and urinary cotinine concentration ≥ 200 ng/mL. Exclusion criteria were positive urine tests for drugs of abuse other than

nicotine or tetrahydrocannabinol, self-report of consuming ≥10 alcoholic drinks per week, any current psychiatric disorder other than TUD as assessed with the Mini International Neuropsychiatric Interview for DSM-5 (Sheehan et al., 1998), history of neurological injury, and using electronic cigarettes, cigars, snuff, or chewing tobacco more than three times a month. Exclusionary criteria for magnetic resonance imaging were left-handedness, claustrophobia, pregnancy, and metallic implants.

2.2. Procedure

The study was conducted at the University of California, Los Angeles (UCLA). During the in-person screening, participants received a complete description of the study procedures, which were approved by the UCLA Institutional Review Board, and provided written informed consent. They were tested in the morning, after overnight abstinence from smoking (~12 hours), verified using a breath monitor (CO <10 ppm or 50% reduction from intake). (See Supplementary Material for details on substance use verification.). The assessments included self-report measures, followed by magnetic resonance spectroscopy, resting-state functional magnetic resonance imaging (fMRI), task-based fMRI, and structural MRI. Subsequently, participants were allowed to smoke and underwent further testing. The current study focuses on the self-report and resting-state fMRI measures prior to smoking. Other aspects of this dataset are reported elsewhere (Ghahremani et al., 2021; Perez Diaz et al., 2021).

2.3. Self-report measures

Prior to the scan, participants completed the 15-item Shiffman-Jarvik Withdrawal Scale (SJWS), each item rated on a 7-point scale (Shiffman and Jarvik, 1976). They also completed the state version of the Spielberger State-Trait Anxiety Inventory (STAI-State) (Spielberger, 1983), a 20-item questionnaire, each item rated on a 4-point scale. Craving was measured using the Craving subscale of the SJWS. Negative affective states were measured using the STAI-State (assessing state anxiety) and the Psychological Symptoms subscale of the SJWS (assessing psychological withdrawal) (see Supplementary Material). During intake, nicotine dependence was measured using the 6-item Fagerström Test for Nicotine Dependence (FTND) (Fagerström, 2011) and trait anxiety was measured using the trait version of the STAI (STAI-Trait) (Spielberger, 1983).

2.4. Neuroimaging data acquisition and preprocessing

Images were acquired on a Siemens 3-Tesla PRISMA MRI scanner using a 32-channel head coil. Resting state echo-planar image (EPI) volumes were acquired over a period of 9 minutes and 50 seconds, using a multiband accelerated EPI pulse sequence (factor 8, isovoxel = 2 mm^3, 104×104 matrix, repetition time (TR) = 800 ms, echo time (TE) = 37 ms, flip angle = 52°, 72 axial slices). During the resting state scan, participants were asked to keep their eyes open and look at a black screen. Structural T1-weighted images were obtained using a magnetization prepared rapid gradient echo (MPRAGE) sequence (isovoxel = 0.8 mm^3, FOV = 240×256 mm^2, TR = 2400 ms, TE = 2.24 ms, flip angle = 8°, 208 sagittal slices).

All analyses were performed on a high-performance computation cluster (Linux CentOS 7) using FSL 5.0.9. The initial pre-processing steps included rigid body realignment to correct for head movements, skull removal, and nonlinear registration to the Montreal Neurological Institute (MNI) template. Motion cleaning and noise reduction were performed using a 24-parameter linear regression model that included six motion parameters, the temporal derivatives of these parameters, and the quadratic of all parameters (Satterthwaite et al., 2013). Mean frame displacement (mFD) and the variance of signal change from the average signal (DVARS) of the raw images were estimated. A null sampling distribution of DVARS was used to identify and flag frames with excessive variance at $p<0.05$ (Afyouni and Nichols, 2018); frames with mFD exceeding 0.45 mm were also flagged. Flagged frames, and frames located in time just prior (t−1) and two after (t+1 and t+2) were included in a censoring temporal mask for data interpolation (see methods in Ghahremani et al., 2021). The interpolated signal was then demeaned, detrended, and filtered using an ideal bandpass filter (0.009–0.08 Hz). Finally, the interpolated timepoints were censored. Four participants with more than 50% frames censored (i.e., those with less than 5 minutes of remaining resting-state data) were excluded. To reduce the contribution from non-neuronal noise, the minimal number of principle components that explained at least 50% of the variance of mean signal extracted from white matter and cerebrospinal fluid were evaluated and regressed out from the signal (aCompCor50, Muschelli et al., 2014). Volumes were then spatially smoothed with a Gaussian filter using a 5-mm FWHM kernel, and each voxel's value was 100-meaned and standardized.

2.5. Seed-based correlation analyses

Seed-based analysis was used because we had a hypothesis about a specific region of the brain, namely the PCC. Two seeds were selected from the set of parcels that represent the DMN in the Cortical Area Parcellation from Resting-State Correlations atlas (Gordon et al., 2016), representing left (parcel #26, 168 mm^3) and right (parcel #186, 96 mm^3) PCC. These two were the only parcels in the atlas that were circumscribed within PCC (see Supplementary Material). For additional triangulation of the association of PCC RSFC with subjective measures, we defined a third PCC seed (4120 mm^3) by building a sphere (10mm radius) around the peak PCC voxel (MNI coordinates: 0, −30, 32) reported in previous studies of DMN and rumination (Lehmann et al., 2016). All three seeds are located in the anterior portion of the PCC and will be referred to as left anterior PCC, right anterior PCC, and medial anterior PCC, respectively. The medial anterior PCC seed shared 2 overlapping voxels with the left and 1 overlapping voxel with the right anterior PCC seeds.

The timeseries from each seed was extracted, and its first normalized eigenvector (mean=100, SD=1) was used as a regressor in a linear regression analysis (using FSL's FILM_GLS in FEAT). To test the specific hypothesis that *connectivity within DMN* is associated with subjective states, we restricted the analyses to voxels within the 34 parcels representing the DMN in the atlas of Gordon et al. (2016). The resulting correlation maps (i.e., Pearson's r maps, because data were previously normalized) were z-transformed and used in second-level general linear model analyses (using FLAME1 in FEAT) with each self-report measure as covariate of interest, and with age and mFD as nuisance variables.

Results were cluster-corrected for multiple comparisons using a voxel-height threshold of $p<0.001$ (Z>3.1) and a cluster-size threshold of $p<0.05$ (Eklund et al., 2016).

2.6. Dual regression analyses

ICA with dual regression was used to address some of the limitations of seed-based analyses, such as seed-selection bias and lack of complexity. The multivariate approach in ICA better captures the brain's complexity by characterizing individual-level spatiotemporal dynamics of each network while controlling for the effect of other networks.

Using FSL's MELODIC tool (Beckmann and Smith, 2004), the preprocessed timeseries were temporally concatenated and submitted to ICA to derive 20 maximally and statistically independent spatial components (Smith et al., 2009). This approach identifies voxels that share similar patterns of signal variation across time (i.e., functional connectivity). Using FSL's dual regression tool (Beckmann et al., 2009), the ICA components were regressed against each participant's preprocessed data to obtain a participant-specific timeseries for each component. Subsequently, these participant-specific timeseries were regressed against each participant's preprocessed data to obtain participant-specific spatial maps. Using FSL's randomize tool (Nichols and Holmes, 2002), the participant-specific spatial maps were entered into separate non-parametric analyses (5000 permutations) with each self-report measure (psychological withdrawal, craving, and state anxiety) as covariate of interest, and with age and mFD as nuisance variables. For each component, this non-parametric analysis results in a p_{corr}-value map, with family-wise error correction for multiple comparisons across voxels and threshold-free cluster enhancement (Smith and Nichols, 2009), and an uncorrected t-value map, indicating how well each voxel's connectivity with the component is associated with the self-report measure of interest. Results are reported for the component that corresponded to the DMN, based on visual inspection and comparison to prior such components (Smith et al., 2009).

For meaningful interpretation and reproducibility, effect-size (R^2) maps were created (Chen et al., 2017) from each p_{corr}-value map using fslmaths with the formula $R^2 = f^2 / (f^2+1)$, where $f^2 = t^2 * (1/N-p)$, and where p = total number of regressors in the model (see Supplementary Material). For reference, according to the convention proposed by Cohen (1988), R^2 of 0.03 to 0.13 is considered a medium effect size.

2.7. Conjunction analyses

To identify the overlap between craving and each analysis of negative affect, conjunction analyses were conducted using FSL's easythresh_conj tool (Nichols, 2007) by creating an intersection of the cluster-corrected z-statistical maps and applying a threshold of Z=3.1 (cluster-corrected at $p<0.05$).

2.8. Analysis of specificity

To test whether PCC RSFC within DMN was specific to abstinence-related subjective states (psychological withdrawal, state anxiety, and craving), additional dual regression and seed-based analyses were conducted with trait anxiety, measured on the STAI-Trait, and with

nicotine dependence, measured on the FTND. Because four participants did not complete the STAI-Trait, the analyses using this trait measure were conducted with N=42.

3. Results

3.1. Self-report

On average, participant scores indicated moderate nicotine dependence (FTND 4.02 ± 2.01) and moderate to high levels of craving (SJWS-Craving 5.18±1.48) (Table 1). Craving was positively correlated with psychological withdrawal (r=0.44, p=0.002) and state anxiety (r=0.34, p=0.021). Confirming that subjective states were induced by abstinence, smoking significantly reduced self-reported craving (−2.3±1.6; p<0.0000001), psychological withdrawal (−0.9±1.2; p<0.00001), and state anxiety (−5.3±9; p<0.0005).

3.2. Resting state connectivity: seed-based correlation

Craving was positively correlated with connectivity of the A) left anterior PCC seed to a more posterior region of the left PCC (Z=4.3; p_{corr}=0.01), B) right anterior PCC seed to a similar posterior region of the left PCC (Z=3.9; p_{corr}=0.03), and C) medial anterior PCC seed to right posterior PCC (Z=3.9; p_{corr}=0.03) (see Figure 1 for additional information). Psychological withdrawal and state anxiety did not significantly correlate with connectivity of any PCC seed to any other part of the DMN. (See Supplementary Material for *post hoc* analyses.)

3.3. Resting state connectivity: dual regression

Psychological withdrawal was positively correlated with DMN RSFC to regions within and outside DMN. These included PCC, precuneus, anterior insula, and striatum (see Table 2 and Figure 2 for statistics and other details). Showing a similar pattern of results, state anxiety was also positively correlated with DMN RSFC to numerous regions, including a PCC cluster that overlapped with the DMN component, as well as striatum and anterior insula subclusters (Table 3, Figure S1). Positive associations between craving and DMN RSFC to frontal operculum / insula (R^2=0.06, p_{corr}=0.06) and PCC (R^2=0.05, p_{corr}=0.08) did not reach statistical significance (Figure S2).

3.4. Conjunction analyses

We tested for overlapping pathways associated with craving and negative affective states by taking the intersection of the cluster-corrected z-static map representing the association of craving with connectivity of the left anterior PCC seed and the cluster-corrected z-static maps representing each of the dual regression analyses with state anxiety and psychological withdrawal. Craving and state anxiety were associated with connectivity of 18 overlapping voxels (144 mm^3) in left posterior PCC (Z=3.89, p_{corr}=0.003) (Figure 3); the association of craving and psychological withdrawal with connectivity of 10 overlapping voxels (80 mm^3) in the same region of left posterior PCC did not reach significance (Z=3.73, p_{corr}=0.152). Conjunction analyses using the association of craving with *right* anterior PCC or *medial* anterior PCC seeds were not significant.

3.5. Analysis of specificity

Neither trait anxiety (p_{corr}>0.9) nor nicotine dependence (p_{corr}>0.2) was associated with connectivity of the DMN component or with connectivity of any of the seeds within DMN (p_{corr}>0.9).

4. Discussion

Following overnight abstinence from smoking, negative affective states (i.e., psychological withdrawal and state anxiety) were associated with RSFC of DMN, not only with reward- and threat-related regions, such as the striatum and anterior insula, but also within DMN itself, particularly involving the PCC. Craving, on the other hand, was associated with RSFC within PCC. Negative affective states and craving were both correlated to within-DMN connectivity of an overlapping region of posterior PCC, suggesting that similar pathways may underlie both subjective states. These posterior PCC clusters were in the same region that has previously been linked to cue-induced reactivity in addiction (Hill-Bowen et al., 2021).

A novel finding here is the association of negative affective states with DMN RSFC during abstinence from smoking. Specifically, psychological withdrawal and state anxiety were each positively correlated to RSFC within DMN (including PCC). They were also correlated with DMN RSFC to regions outside DMN, such as the striatum. Greater RSFC *within* DMN may reflect greater mind-wandering and rumination (Christoff et al., 2016; Zhou et al., 2020), both of which may contribute to negative psychological states (Killingsworth and Gilbert, 2010; Nolen-Hoeksema et al., 2008). DMN-striatum coupling, on the other hand, may reflect obsessive thinking about the upcoming opportunity to smoke. It may be an attempt to mind-wander away from unpleasant states, akin to coupling of DMN with midbrain analgesia-related centers observed in mind-wandering away from pain (Kucyi et al., 2013). Another possibility is that DMN-striatum coupling is a way of compensating for deficient reward function (e.g., anhedonia), as reported in subthreshold depression (Hwang et al., 2016). This interpretation is relevant considering the high comorbidity of depression and smoking (Leventhal and Zvolensky, 2015).

Our seed-based correlational results are consistent with prior reports that cigarette craving correlates positively with RSFC within DMN. Scores on the Questionnaire of Smoking Urges have shown a positive correlation with RSFC within MPFC (Janes et al., 2014; Zhao et al., 2019), and scores on the Visual Analog Scale of craving have shown a positive correlation with RSFC between MPFC and precuneus (Huang et al., 2014). While none of these studies reported connectivity with PCC specifically, none used PCC-specific seed-based analyses as done in the current study. Janes et al. (2014) used a dual regression analysis. However, in our dual regression analyses, correlations of DMN connectivity with craving did not reach significance (p_{corr}=0.08). Discrepancies between our findings and these prior reports may be due to differences in duration of abstinence, self-report instruments, or sample characteristics, such as sex/gender composition (100% male in Zhao et al., 2019). Additionally, replicability of findings is compromised by sample size (n<18 in Huang et al., 2014; Janes et al., 2014).

4.1. Limitations

A potential limitation of this study is that the two different analysis pipelines (seed-based correlations and dual regression) did not produce perfectly matched results. However, the discrepancy is not surprising, given that one method relies on a single seed region, whereas the other integrates data across multiple distributed networks. These fundamental differences in methodologies make it more compelling that both pipelines identified positive associations between withdrawal-related subjective states and RSFC of posterior PCC within DMN. In the dual regression analysis, the positive association between craving and within-DMN connectivity of PCC did not quite reach significance (p_{corr}=0.08), but it was consistent with the significant effect in the seed-based analysis (p_{corr}<0.05). Overall, the results indicate that although the circuits for craving and negative affective states are not identical, these subjective states are both associated with greater within-DMN connectivity of PCC. Another limitation is that the instruments used to assess negative affect (i.e., SJWS and STAI-State) provide relatively limited coverage of the construct (e.g., no items assessing sadness/dysphoria). Future studies can assess broader coverage of these states.

4.2. Implications

A unique contribution of the current study is that it tested both craving and negative affective states during abstinence. Our results indicate that abstinence-related craving and negative affective states are both positively associated with RSFC within DMN, particularly involving PCC, but in different ways. One implication of similar (albeit non-identical) pathways underlying craving and negative affect is that interventions that are effective in regulating negative affect may be adapted to regulate craving (e.g., Ghahremani et al., 2018; Tabibnia et al., 2014) and vice-versa (Brewer and Roy, 2021). Given the comorbidity of anxiety and smoking (Leventhal and Zvolensky, 2015), and the roles of craving and negative subjective states in smoking cessation (Killen and Fortmann, 1997; Leventhal and Zvolensky, 2015; Piper et al., 2011; Zhou et al., 2009), future studies can evaluate DMN (particularly the PCC) as a particularly effective therapeutic target or biomarker for intervention in TUD, because this region may underlie both subjective states. Potential interventions may include targeted brain stimulation, such as low-intensity focused ultrasound (Fomenko et al., 2018), behavioral techniques, or medications. For example, prior work has identified the PCC as a plausible target of meditation with neurofeedback for treatment of anxiety and addiction (Brewer and Garrison, 2014). In addition to mindfulness meditation (Fox et al., 2016; Tang et al., 2015), other interventions that diminish DMN hyperactivity or hyperconnectivity (reviewed in Tabibnia, 2020) may also be effective. These include exposure to nature (Norwood et al., 2019), or treatment with ketamine (Scheidegger et al., 2012) or psychedelics (Carhart-Harris et al., 2012; Palhano-Fontes et al., 2015).

The finding that nicotine dependence is not associated with RSFC of PCC within DMN is consistent with prior neuroimaging studies using the FTND (Claus and Weywadt, 2020; Tang et al., 2016; Vergara et al., 2017; Yu et al., 2013). Together with the finding that trait anxiety is not associated with PCC connectivity, these results are consistent with the possibility that PCC connectivity is specifically associated with abstinence-related subjective states (psychological withdrawal, state anxiety, and craving), rather than with more stable aspects of negative affect or nicotine dependence. Association of PCC with state-like rather

than trait-like processes would further highlight the potential of this region as a therapeutic target, linking it to underlying processes that are amenable to change.

5. Conclusions

This study identified a role of PCC in negative affective states and craving, subjective states that reinforce smoking. These findings raise the possibility that behavioral (e.g., mindfulness), pharmaceutical (e.g., ketamine), or neural (e.g., low-intensity focused ultrasound) interventions that disrupt this DMN activity may be particularly helpful in preventing recurrence of smoking. However, clinical trials are needed to confirm these practical implications.

Supplementary Material

Refer to Web version on PubMed Central for supplementary material.

REFERENCES

Afyouni S, Nichols TE, 2018. Insight and inference for DVARS. NeuroImage 172, 291–312. [PubMed: 29307608]

Ameringer KJ, Leventhal AM, 2010. Applying the Tripartite Model of Anxiety and Depression to Cigarette Smoking: An Integrative Review. Nicotine & Tobacco Research 12, 1183–1194. [PubMed: 21036959]

Andrews-Hanna JR, Smallwood J, Spreng RN, 2014. The default network and self-generated thought: component processes, dynamic control, and clinical relevance. Annals of the New York Academy of Sciences 1316, 29–52. [PubMed: 24502540]

Beckmann CF, Mackay CE, Filippini N, Smith SM, 2009. Group comparison of resting-state FMRI data using multi-subject ICA and dual regression. NeuroImage 47, S148.

Beckmann CF, Smith SM, 2004. Probabilistic Independent Component Analysis for Functional Magnetic Resonance Imaging. IEEE Transactions on Medical Imaging 23, 137–152. [PubMed: 14964560]

Berman MG, Misic B, Buschkuehl M, Kross E, Deldin PJ, Peltier S, Churchill NW, Jaeggi SM, Vakorin V, McIntosh AR, Jonides J, 2014. Does resting-state connectivity reflect depressive rumination? A tale of two analyses. NeuroImage 103, 267–279. [PubMed: 25264228]

Botvinik-Nezer R, Holzmeister F, Camerer CF, Dreber A, Huber J, Johannesson M, Kirchler M, Iwanir R, Mumford JA, Adcock RA, 2020. Variability in the analysis of a single neuroimaging dataset by many teams. Nature 582, 84–88. [PubMed: 32483374]

Brewer JA, Garrison KA, 2014. The posterior cingulate cortex as a plausible mechanistic target of meditation: findings from neuroimaging. Annals of the New York Academy of Sciences 1307, 19–27. [PubMed: 24033438]

Brewer JA, Roy A, 2021. Can Approaching Anxiety Like a Habit Lead to Novel Treatments? American Journal of Lifestyle Medicine 15, 489–494. [PubMed: 34646095]

Buckner RL, DiNicola LM, 2019. The brain's default network: updated anatomy, physiology and evolving insights. Nature reviews. Neuroscience 20, 593–608. [PubMed: 31492945]

Carhart-Harris RL, Erritzoe D, Williams T, Stone JM, Reed LJ, Colasanti A, Tyacke RJ, Leech R, Malizia AL, Murphy K, 2012. Neural correlates of the psychedelic state as determined by fMRI studies with psilocybin. Proceedings of the National Academy of Sciences 109, 2138–2143.

Charney DS, 2004. Psychobiological mechanisms of resilience and vulnerability. American Journal of Psychiatry 161, 195–216. [PubMed: 14754765]

Chen G, Taylor PA, Cox RW, 2017. Is the statistic value all we should care about in neuroimaging? NeuroImage 147, 952–959. [PubMed: 27729277]

Christoff K, Irving ZC, Fox KC, Spreng RN, Andrews-Hanna JR, 2016. Mind-wandering as spontaneous thought: a dynamic framework. Nature reviews. Neuroscience 17, 718–731. [PubMed: 27654862]

Claus ED, Weywadt CR, 2020. Resting-State Connectivity in Former, Current, and Never Smokers. Nicotine & tobacco research : official journal of the Society for Research on Nicotine and Tobacco 22, 180–187. [PubMed: 30590742]

Cohen J, 1988. Statistical power analysis for the behavioral sciences, 2nd ed. Laurence Erlbaum Associates, Hillsdale, NJ.

Cole DM, Beckmann CF, Long CJ, Matthews PM, Durcan MJ, Beaver JD, 2010. Nicotine replacement in abstinent smokers improves cognitive withdrawal symptoms with modulation of resting brain network dynamics. NeuroImage 52, 590–599. [PubMed: 20441798]

Creamer MR, Wang TW, Babb S, Cullen KA, Day H, Willis G, Jamal A, Neff L, 2019. Tobacco product use and cessation indicators among adults—United States, 2018. Morbidity and Mortality Weekly Report 68, 1013.

Ding X, Lee SW, 2013. Changes of functional and effective connectivity in smoking replenishment on deprived heavy smokers: a resting-state FMRI study. PloS one 8, e59331. [PubMed: 23527165]

Eklund A, Nichols TE, Knutsson H, 2016. Cluster failure: Why fMRI inferences for spatial extent have inflated false-positive rates. Proceedings of the national academy of sciences 113, 7900–7905.

Fagerström K, 2011. Determinants of tobacco use and renaming the FTND to the Fagerström Test for Cigarette Dependence. Nicotine & tobacco research 14, 75–78. [PubMed: 22025545]

Fatseas M, Serre F, Swendsen J, Auriacombe M, 2018. Effects of anxiety and mood disorders on craving and substance use among patients with substance use disorder: An ecological momentary assessment study. Drug and alcohol dependence 187, 242–248. [PubMed: 29684892]

Fomenko A, Neudorfer C, Dallapiazza RF, Kalia SK, Lozano AM, 2018. Low-intensity ultrasound neuromodulation: An overview of mechanisms and emerging human applications. Brain Stimulation 11, 1209–1217. [PubMed: 30166265]

Fox KC, Dixon ML, Nijeboer S, Girn M, Floman JL, Lifshitz M, Ellamil M, Sedlmeier P, Christoff K, 2016. Functional neuroanatomy of meditation: A review and meta-analysis of 78 functional neuroimaging investigations. Neuroscience and biobehavioral reviews 65, 208–228. [PubMed: 27032724]

Ghahremani DG, Faulkner P, Cox CM, London ED, 2018. Behavioral and neural markers of cigarette-craving regulation in young-adult smokers during abstinence and after smoking. Neuropsychopharmacology : official publication of the American College of Neuropsychopharmacology 43, 1616–1622. [PubMed: 29472643]

Ghahremani DG, Pochon J-B, Perez Diaz M, Tyndale RF, Dean AC, London ED, 2021. Functional connectivity of the anterior insula during withdrawal from cigarette smoking. Neuropsychopharmacology : official publication of the American College of Neuropsychopharmacology 46, 2083–2089. [PubMed: 34035468]

Gitchell JG, Shiffman S, Sembower MA, 2017. Trends in serious quit attempts in the United States, 2009–14. Addiction 112, 897–900. [PubMed: 27933678]

Giuliani NR, Berkman ET, 2015. Craving Is an Affective State and Its Regulation Can Be Understood in Terms of the Extended Process Model of Emotion Regulation. Psychological Inquiry 26, 48–53. [PubMed: 25780321]

Gordon EM, Laumann TO, Adeyemo B, Huckins JF, Kelley WM, Petersen SE, 2016. Generation and Evaluation of a Cortical Area Parcellation from Resting-State Correlations. Cerebral Cortex 26, 288–303. [PubMed: 25316338]

Hill-Bowen LD, Riedel MC, Poudel R, Salo T, Flannery JS, Camilleri JA, Eickhoff SB, Laird AR, Sutherland MT, 2021. The cue-reactivity paradigm: An ensemble of networks driving attention and cognition when viewing drug and natural reward-related stimuli. Neuroscience & Biobehavioral Reviews 130, 201–213. [PubMed: 34400176]

Huang W, King JA, Ursprung WW, Zheng S, Zhang N, Kennedy DN, Ziedonis D, DiFranza JR, 2014. The development and expression of physical nicotine dependence corresponds to structural and functional alterations in the anterior cingulate-precuneus pathway. Brain Behav 4, 408–417. [PubMed: 24944870]

Hwang JW, Xin SC, Ou YM, Zhang WY, Liang YL, Chen J, Yang XQ, Chen XY, Guo TW, Yang XJ, Ma WH, Li J, Zhao BC, Tu Y, Kong J, 2016. Enhanced default mode network connectivity with ventral striatum in subthreshold depression individuals. Journal of Psychiatric Research 76, 111–120. [PubMed: 26922247]

Janes AC, Farmer S, Frederick B, Nickerson LD, Lukas SE, 2014. An increase in tobacco craving is associated with enhanced medial prefrontal cortex network coupling. PloS one 9, e88228. [PubMed: 24505440]

Killen JD, Fortmann SP, 1997. Craving is associated with smoking relapse: findings from three prospective studies. Experimental and clinical psychopharmacology 5, 137. [PubMed: 9234050]

Killingsworth MA, Gilbert DT, 2010. A Wandering Mind Is an Unhappy Mind. Science 330, 932–932. [PubMed: 21071660]

Knapp KS, Bunce SC, Brick TR, Deneke E, Cleveland HH, 2021. Daily associations among craving, affect, and social interactions in the lives of patients during residential opioid use disorder treatment. Psychology of Addictive Behaviors 35, 609–620. [PubMed: 33090811]

Kucyi A, Salomons TV, Davis KD, 2013. Mind wandering away from pain dynamically engages antinociceptive and default mode brain networks. Proceedings of the National Academy of Sciences 110, 18692–18697.

Kunas SL, Stuke H, Heinz A, Ströhle A, Bermpohl F, 2021. Evidence for a hijacked brain reward system but no desensitized threat system in quitting motivated smokers: An fMRI study. Addiction.

Lehmann M, Seifritz E, Henning A, Walter M, Boker H, Scheidegger M, Grimm S, 2016. Differential effects of rumination and distraction on ketamine induced modulation of resting state functional connectivity and reactivity of regions within the default-mode network. Social cognitive and affective neuroscience 11, 1227–1235. [PubMed: 27075438]

Leventhal AM, Zvolensky MJ, 2015. Anxiety, depression, and cigarette smoking: A transdiagnostic vulnerability framework to understanding emotion–smoking comorbidity. Psychological bulletin 141, 176–212. [PubMed: 25365764]

Li Y, Yuan K, Bi Y, Guan Y, Cheng J, Zhang Y, Shi S, Lu X, Yu D, Tian J, 2017. Neural correlates of 12-h abstinence-induced craving in young adult smokers: a resting-state study. Brain Imaging Behav 11, 677–684. [PubMed: 26995747]

Li Y, Zhuang K, Yi Z, Wei D, Sun J, Qiu J, 2020. The trait and state negative affect can be separately predicted by stable and variable resting-state functional connectivity. Psychological medicine, 1–11.

Messer S, Siegel A, Bertin L, Erblich J, 2018. Sex differences in affect-triggered lapses during smoking cessation: A daily diary study. Addictive behaviors 87, 82–85. [PubMed: 29966963]

Muschelli J, Nebel MB, Caffo BS, Barber AD, Pekar JJ, Mostofsky SH, 2014. Reduction of motion-related artifacts in resting state fMRI using aCompCor. NeuroImage 96, 22–35. [PubMed: 24657780]

Nelson BD, McGowan SK, Sarapas C, Robison-Andrew EJ, Altman SE, Campbell ML, Gorka SM, Katz AC, Shankman SA, 2013. Biomarkers of threat and reward sensitivity demonstrate unique associations with risk for psychopathology. Journal of Abnormal Psychology 122, 662–671. [PubMed: 24016008]

Nichols T, 2007. Easythresh_conj—quick method of getting conjunction stats outside of Feat [web page].

Nichols TE, Holmes AP, 2002. Nonparametric permutation tests for functional neuroimaging: a primer with examples. Human brain mapping 15, 1–25. [PubMed: 11747097]

Nolen-Hoeksema S, Wisco BE, Lyubomirsky S, 2008. Rethinking Rumination. Perspectives on psychological science : a journal of the Association for Psychological Science 3, 400–424. [PubMed: 26158958]

Norwood MF, Lakhani A, Maujean A, Zeeman H, Creux O, Kendall E, 2019. Brain activity, underlying mood and the environment: A systematic review. Journal of Environmental Psychology, 101321.

Palhano-Fontes F, Andrade KC, Tofoli LF, Santos AC, Crippa JA, Hallak JE, Ribeiro S, de Araujo DB, 2015. The psychedelic state induced by ayahuasca modulates the activity and connectivity of the default mode network. PloS one 10, e0118143. [PubMed: 25693169]

Pariyadath V, Stein EA, Ross TJ, 2014. Machine learning classification of resting state functional connectivity predicts smoking status. Frontiers in human neuroscience 8, 425. [PubMed: 24982629]

Perez Diaz M, Pochon J-B, Ghahremani DG, Dean AC, Faulkner P, Petersen N, Tyndale RF, Donis A, Paez D, Cahuantzi C, Hellemann GS, London ED, 2021. Sex Differences in the Association of Cigarette Craving With Insula Structure. International Journal of Neuropsychopharmacology 24, 624–633. [PubMed: 33830218]

Piper ME, Cook JW, Schlam TR, Jorenby DE, Baker TB, 2011. Anxiety diagnoses in smokers seeking cessation treatment: relations with tobacco dependence, withdrawal, outcome and response to treatment. Addiction 106, 418–427. [PubMed: 20973856]

Raichle ME, MacLeod AM, Snyder AZ, Powers WJ, Gusnard DA, Shulman GL, 2001. A default mode of brain function. Proceedings of the National Academy of Sciences 98, 676–682.

Reddan MC, Lindquist MA, Wager TD, 2017. Effect Size Estimation in Neuroimaging. JAMA Psychiatry 74, 207. [PubMed: 28099973]

Renner F, Siep N, Arntz A, van de Ven V, Peeters FPML, Quaedflieg CWEM, Huibers MJH, 2017. Negative mood-induction modulates default mode network resting-state functional connectivity in chronic depression. Journal of affective disorders 208, 590–596. [PubMed: 27810271]

Satterthwaite TD, Elliott MA, Gerraty RT, Ruparel K, Loughead J, Calkins ME, Eickhoff SB, Hakonarson H, Gur RC, Gur RE, 2013. An improved framework for confound regression and filtering for control of motion artifact in the preprocessing of resting-state functional connectivity data. NeuroImage 64, 240–256. [PubMed: 22926292]

Scheidegger M, Walter M, Lehmann M, Metzger C, Grimm S, Boeker H, Boesiger P, Henning A, Seifritz E, 2012. Ketamine decreases resting state functional network connectivity in healthy subjects: implications for antidepressant drug action.

Sheehan DV, Lecrubier Y, Sheehan KH, Amorim P, Janavs J, Weiller E, Hergueta T, Baker R, Dunbar GC, 1998. The Mini-International Neuropsychiatric Interview (MINI): the development and validation of a structured diagnostic psychiatric interview for DSM-IV and ICD-10. The Journal of clinical psychiatry.

Shiffman SM, Jarvik ME, 1976. Smoking withdrawal symptoms in two weeks of abstinence. Psychopharmacology 50, 35–39. [PubMed: 827760]

Sinha R, 2011. New Findings on Biological Factors Predicting Addiction Relapse Vulnerability. Current psychiatry reports 13, 398–405. [PubMed: 21792580]

Smith SM, Fox PT, Miller KL, Glahn DC, Fox PM, Mackay CE, Filippini N, Watkins KE, Toro R, Laird AR, 2009. Correspondence of the brain's functional architecture during activation and rest. Proceedings of the national academy of sciences 106, 13040–13045.

Smith SM, Nichols TE, 2009. Threshold-free cluster enhancement: addressing problems of smoothing, threshold dependence and localisation in cluster inference. NeuroImage 44, 83–98. [PubMed: 18501637]

Spielberger C, 1983. Manual for the state-trait anxiety inventory. Spieberger CD (Ed). STAI Manual. Palo Alto Calif Consulting. Psychologist Press.

Tabibnia G, 2020. An Affective Neuroscience Model of Boosting Resilience in Adults. Neuroscience and biobehavioral reviews 115, 321–350. [PubMed: 32522489]

Tabibnia G, Creswell JD, Kraynak T, Westbrook C, Julson E, Tindle HA, 2014. Common prefrontal regions activate during self-control of craving, emotion, and motor impulses in smokers. Clinical psychological science : a journal of the Association for Psychological Science 2, 611–619. [PubMed: 25485181]

Tang R, Razi A, Friston KJ, Tang YY, 2016. Mapping Smoking Addiction Using Effective Connectivity Analysis. Frontiers in human neuroscience 10, 195. [PubMed: 27199716]

Tang YY, Holzel BK, Posner MI, 2015. The neuroscience of mindfulness meditation. Nature reviews. Neuroscience 16, 213–225. [PubMed: 25783612]

Tye KM, Prakash R, Kim S-Y, Fenno LE, Grosenick L, Zarabi H, Thompson KR, Gradinaru V, Ramakrishnan C, Deisseroth K, 2011. Amygdala circuitry mediating reversible and bidirectional control of anxiety. Nature 471, 358–362. [PubMed: 21389985]

Vergara VM, Liu J, Claus ED, Hutchison K, Calhoun V, 2017. Alterations of resting state functional network connectivity in the brain of nicotine and alcohol users. NeuroImage 151, 45–54. [PubMed: 27864080]

Volkow ND, Morales M, 2015. The Brain on Drugs: From Reward to Addiction. Cell 162, 712–725. [PubMed: 26276628]

Watson NL, DeMarree KG, Cohen LM, 2018. Cigarette craving and stressful social interactions: The roles of state and trait social anxiety and smoking to cope. Drug and alcohol dependence 185, 75–81. [PubMed: 29428323]

Whitfield-Gabrieli S, Ford JM, 2012. Default mode network activity and connectivity in psychopathology. Annual review of clinical psychology 8, 49–76.

WHO, 2020. Fact Sheet: Tobacco.

Wolitzky-Taylor K, Schiffman J, 2019. Predictive Associations Among the Repeated Measurements of Anxiety, Depression, and Craving in a Dual Diagnosis Program. Journal of Dual Diagnosis 15, 140–146. [PubMed: 30982462]

Yu R, Zhao L, Tian J, Qin W, Wang W, Yuan K, Li Q, Lu L, 2013. Regional homogeneity changes in heavy male smokers: a resting-state functional magnetic resonance imaging study. Addiction biology 18, 729–731. [PubMed: 21812873]

Zhang R, Volkow ND, 2019. Brain default-mode network dysfunction in addiction. NeuroImage 200, 313–331. [PubMed: 31229660]

Zhang W, Llera A, Hashemi MM, Kaldewaij R, Koch SBJ, Beckmann CF, Klumpers F, Roelofs K, 2020. Discriminating stress from rest based on resting-state connectivity of the human brain: A supervised machine learning study. Human brain mapping 41, 3089–3099. [PubMed: 32293072]

Zhao S, Li Y, Li M, Wang R, Bi Y, Zhang Y, Lu X, Yu D, Yang L, Yuan K, 2019. 12-h abstinence-induced functional connectivity density changes and craving in young smokers: a resting-state study. Brain Imaging Behav 13, 953–962. [PubMed: 29926324]

Zhou H-X, Chen X, Shen Y-Q, Li L, Chen N-X, Zhu Z-C, Castellanos FX, Yan C-G, 2020. Rumination and the default mode network: Meta-analysis of brain imaging studies and implications for depression. NeuroImage 206, 116287. [PubMed: 31655111]

Zhou X, Nonnemaker J, Sherrill B, Gilsenan AW, Coste F, West R, 2009. Attempts to quit smoking and relapse: factors associated with success or failure from the ATTEMPT cohort study. Addictive behaviors 34, 365–373. [PubMed: 19097706]

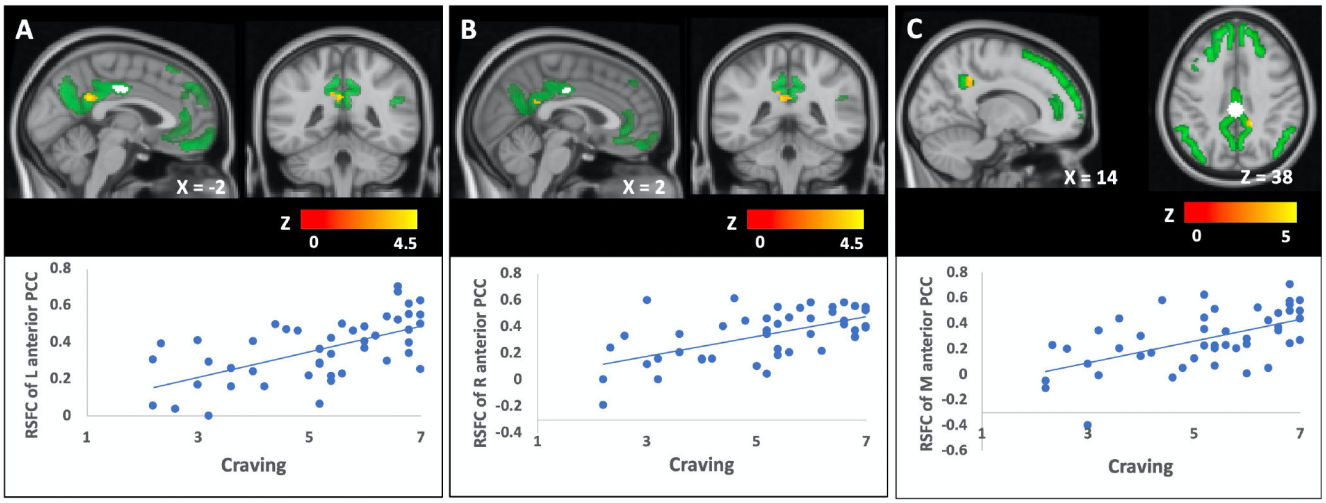

Figure 1.

Association between craving (measured on the SJWS craving subscale) and resting state functional connectivity of A) the left (L) anterior PCC seed with a left posterior PCC cluster (peak MNI coordinates = [−2, −46, 28]; $Z = 4.3$; $p_{corr} = 0.01$; k = 57); B) the right (R) anterior PCC seed with a similar left posterior PCC cluster (peak MNI coordinates = [−6, −42, 24]; $Z = 3.9$; $p_{corr} = 0.03$; k = 46); and C) the medial (M) anterior PCC seed with a right posterior PCC cluster (peak MNI coordinates = [16, −44, 38]; $Z = 3.9$; $p_{corr} = 0.03$; k = 42). Results are from hypothesis-driven seed-based correlation analyses restricted to a search space within the Gordon Atlas DMN (shown in green). The significant cluster is shown in yellow. The seed is shown in white. Upper panels show thresholded statistical maps of the correlation (cluster-corrected at voxel-height threshold of $Z > 3.1$ and cluster-size threshold of $p < 0.05$), in neurological convention. For illustrative purposes, lower panels show scatterplots of relationships between craving (rated on a scale of 1 to 7) and PCC connectivity (r value).

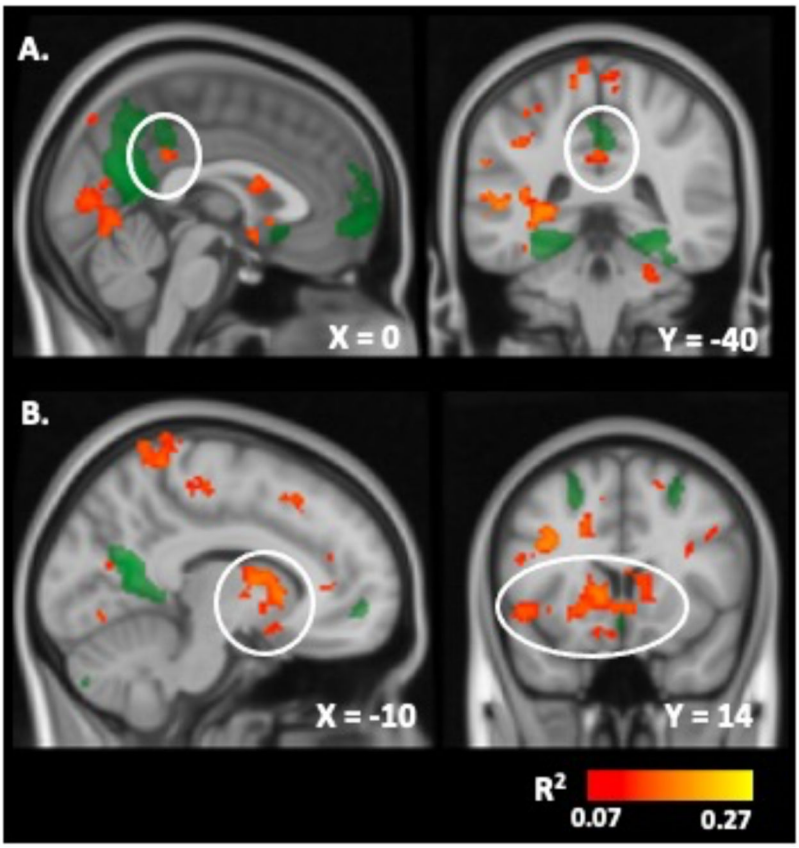

Figure 2.

Association between psychological withdrawal (measured on the SJWS psychological symptoms subscale) and resting state functional connectivity of the DMN component with several regions, including A) posterior cingulate cortex (peak MNI coordinates = [0, −40, 32]; $R^2 = 0.10$; $p_{corr} = 0.02$), and B) a cluster comprised of the striatum, nucleus accumbens, subcallosal cortex, and anterior insula (peak MNI coordinates = [−10, 14, 2]; $R^2 = 0.14$; $p_{corr} = 0.006$). Effect size maps (R^2) are shown, based on results from the dual regression analysis. For visualization purposes, the DMN component is shown in green and maps are shown in neurological convention and rendered at $0.07 < R^2 < 0.27$ and $k > 20$.

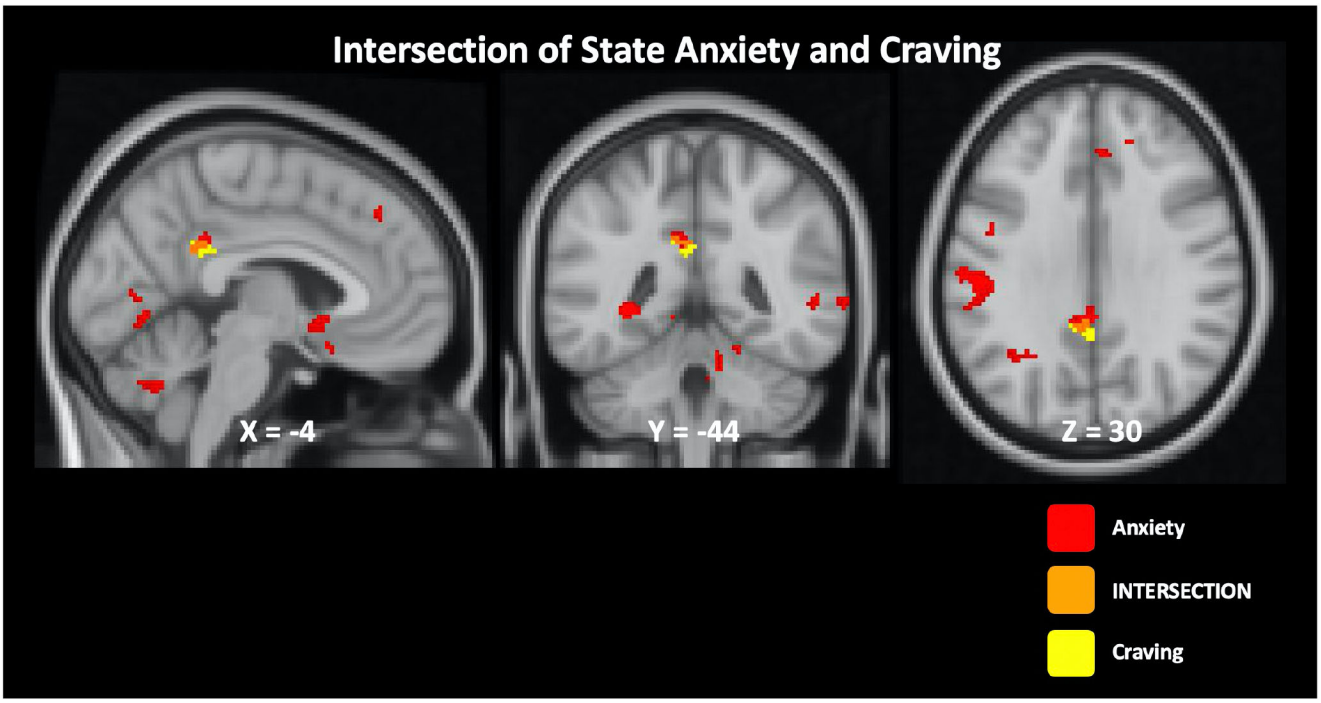

Figure 3.

The z-statistic maps of DMN RSFC associated with craving (yellow) and state anxiety (red). The maps show the overlap (orange) between the association of state anxiety with connectivity of the DMN component and the association of craving with connectivity of the left anterior PCC seed (Gordon #26). These z-statistic maps, presented in neurological convention, are cluster-corrected at a voxel-height threshold of $Z > 3.1$ and a cluster-size threshold of $p < 0.05$.

Table 1.

Sample characteristics and self-reported data (n = 46, unless noted otherwise)

	Percent	Range	Mean	(SD)
Age (years)		18-45	33	(7.2)
Female	50%			
Ethnicity				
Hispanic	13.0%			
Non-Hispanic	82.6%			
Unknown	4.3%			
Race				
African-American	23.9%			
Asian	2.2%			
Caucasian	58.7%			
Mixed	8.7%			
Pacific Islander	4.3%			
Unknown	2.2%			
FTND		0-8	4.02	(2.01)
SJWS-Total		21-97	56.41	(16.31)
SJWS-Psychological		1-7	3.57	(1.41)
SJWS-Craving		2-7	5.18	(1.48)
STAI-State		20-72	35	(11.05)
STAI-Trait (n = 42)		20-61	31	(8.15)

*Note*s: SD = standard deviation; FTND = Fagerström Test for Nicotine Dependence (6 items, possible score range 0-10); SJWS = Shiffman Jarvik Withdrawal Scale (15 items, total score range 15-105; subscale score range 1-7); STAI = State Trait Anxiety Inventory (20 items, score range 20-80).

Table 2.

Association of psychological withdrawal (measured on the SJWS psychological symptoms subscale) with RSFC of the DMN component.

Regions	R^2	p_{corr}	X	Y	Z	k
Supramarginal g, postcentral g, parietal operculum	0.237	0.000	−54	−34	36	3477
Lateral occipital	0.146	0.005	−26	−74	60	271
Precentral g / postcentral g	0.142	0.006	36	−22	56	77
Caudate, accumbens, putamen, subcallosal ctx, anterior insula	0.141	0.006	−10	14	2	1170
Posterior STG	0.141	0.006	60	−14	−6	194
Anterior Insula	0.129	0.008	−26	26	8	365
Precentral g / postcentral g	0.109	0.014	−12	−22	56	114
Lingual g	0.105	0.016	−6	−70	0	758
Postcentral g, supramarginal g	0.102	0.017	52	−24	48	113
PCC	0.101	0.018	0	−40	32	42
MFG	0.100	0.018	20	0	40	135
MTG / angular g	0.096	0.020	66	−46	2	69
SFG	0.096	0.021	22	18	50	222
Cerebellum	0.094	0.021	40	−48	−28	152
Postcentral g, precuneus	0.094	0.022	8	−46	72	98
Precuneus	0.094	0.022	2	−78	48	36
Precentral g / postcentral g	0.091	0.024	62	20	26	40
Frontal pole	0.089	0.025	−18	54	14	135
MFG	0.088	0.025	48	26	44	75
Central opercular ctx / insula	0.088	0.025	−34	4	14	49
Anterior paracingulate ctx	0.088	0.025	6	48	24	230
Cerebellum	0.086	0.024	−36	−72	−28	40
MFG	0.084	0.028	−36	30	32	69
Mid insula	0.082	0.029	−34	−12	8	29
Planum polare / inferior Insula	0.082	0.030	−40	−14	−8	26
Cerebellum	0.081	0.031	20	−44	−18	23
Supramarginal g / postcentral g	0.081	0.031	60	−24	40	21
Temporal occipital fusiform / lingual g	0.080	0.031	−22	−62	−14	25
Posterior MTG	0.080	0.032	−58	−58	8	141
Angular g / supramarginal g	0.077	0.034	−50	−56	48	58
Planum temporale	0.077	0.034	60	−28	12	35
Occipital pole	0.077	0.034	16	−98	16	31
Cerebellum	0.075	0.036	48	−64	−30	25
IFG *pars opercularis*	0.073	0.038	34	12	26	28
SMA / precentral g	0.072	0.039	6	−12	52	25
SFG	0.071	0.040	8	38	60	24
MFG	0.066	0.046	44	12	34	27

Notes: Results are from the dual regression analysis. Only clusters with k > 20 are listed. Effect sizes are reported for the peak voxel. Effect sizes for all the voxels can be obtained from the contrast map available at https://identifiers.org/neurovault.collection:13775.

Table 3.

Association of state anxiety (measured on the STAI-State) with RSFC of the DMN component.

Regions	R^2	p_{corr}	X	Y	Z	k
Supramarginal g, Heschel's g, postcentral g, central operculum, IFG, MFG	0.261	0.0002	−52	−26	30	1654
L Caudate / putamen / accumbens, L anterior insula, L OFC	0.135	0.0070	−12	14	0	327
Frontal pole	0.156	0.0040	−18	56	14	185
L Subcallosal cortex, R caudate, R accumbens	0.117	0.0114	−10	10	−14	143
Lateral occipital	0.131	0.0078	−26	−72	60	127
MTG / angular g	0.128	0.0086	−62	−58	8	75
Lateral ventricle	0.131	0.0114	2	6	18	54
STG, MTG, Heschel's, precuneus	0.162	0.0034	60	−14	−6	6916
SMA, precuneus	0.122	0.0102	10	−8	52	4446
Frontal pole, precuneus	0.084	0.0284	10	62	30	351
Precentral / postcentral, precuneus / PCC	0.080	0.0312	10	−30	52	284
PCC	0.097	0.0200	0	−40	32	257
Lateral occipital / precuneus	0.080	0.0316	14	−66	52	158
Occipital pole	0.074	0.0370	−24	−94	18	122
Occipital pole	0.076	0.0348	−10	−94	18	115
Frontal pole	0.071	0.0398	20	50	2	85
ACC / subcallosal ctx	0.071	0.0402	0	34	−4	55
Posterior insula	0.071	0.0408	36	−10	12	35
Occipital pole	0.066	0.0460	10	−96	26	34

Notes: Results are from the dual regression analysis. Only clusters with k > 20 are listed. Effect sizes are reported for the peak voxel. Effect sizes for all the voxels can be obtained from the contrast map available at https://identifiers.org/neurovault.collection:13775.